*Progress In Electromagnetics Research M, Vol. 48, 37–44, 2016*

# A Passive Suppressing Jamming Method for FMCW SAR Based on Micromotion Modulation

**Jia-Bing Yan*, Ying Liang, Yong-An Chen, Qun Zhang, and Li Sun**

**Abstract**—The frequency-modulated continuous wave (FMCW) synthetic aperture radar (SAR) has the properties of compact size, lightweight, low cost and low power dissipation, which provides great potential in the application of small platforms such as unmanned aerial vehicle (UAV). The imaging characteristics of rotary target for FMCW SAR are analysed based on the construction of echo signal model. Further, a passive suppressing jamming method for FMCW SAR based on micromotion modulation is proposed. This method makes use of rotary corner reflectors to form jamming strips in range and azimuth, and then the target screened is protected effectively. The choice of parameters of rotary corner reflectors is discussed in detail. Finally, some simulations are given to validate the theoretical derivation and the effectiveness of method.

## 1. INTRODUCTION

Compared to conventional pulse-synthetic aperture radar (pulse-SAR), frequency-modulated continuous wave (FMCW) SAR takes the advantages of compact size, lightweight, low cost and low power dissipation [1–3]. The "dechirp" processing is adopted in its receiver, where frequency mixing is conducted between echo signal and reference signal, and difference-frequency signal of narrow bandwidth is generated, thus reducing the requirements for video receiver, A/D sampling equipment and signal processing speed [4]. Meanwhile, the large time-bandwidth product of FMCW SAR makes it difficult for conventional reconnaissance aircraft to intercept and capture, owning favorable low probability of interception [5]. These features make it fairly applicable for military small-sized platform, which greatly improves the capability of SAR in military applications. Researches on FMCW SAR have been widely conducted in many countries [6–8], among them the MicroSAR system developed by the Brigham Young University in U.S. adopting FMCW SAR only weighs about 2 kg [8]. How to protect one's own important targets from the enemy's SAR recognition and improve one's own anti-jamming ability of SAR has always been an important topic for jamming technology and SAR imaging research.

The passive suppressing jamming for SAR is mainly realized through placing jamming targets with large radar cross section (RCS) such as corner reflector and tin foil around the screened targets, thus submerging the screened targets in strong side lobe of jamming targets. Passive suppressing jamming for SAR based on micromotion modulation further adopts the rotation of corner reflectors to form jamming stripes in range and azimuth. Some researches focused on passive and active jamming method for SAR based on micromotion modulation has appeared in the past few years [9, 10]. In [9] a new passive barrage jamming method for SAR is proposed using the rotating angular reflectors, and the selection of the key parameter of the rotating angular reflectors is discussed in detail. Ref. [10] proposed an active jamming method for SAR based on micromotion. Furthermore, in [11] and [12] the SAR imaging characteristics of rotating targets are analyzed, which can also provide a reference for the jamming method based on micromotion.

*Received 28 April 2015, Accepted 13 April 2016, Scheduled 20 April 2016*
* Corresponding author: Jia-Bing Yan (274956059@qq.com).
The authors are with the School of Information and Navigation, AFEU, Xi'an 710077, China.

However, the aforementioned researches mainly studied the jamming method for pulse-SAR, while the passive jamming method for FMCW SAR based on micromotion modulation has not been studied. To guarantee low transmission power, FMCW SAR signal usually adopts long pulse duration, therefore the change of range with the continuous movement of carrier aircraft should be considered in the FMCW SAR signal processing, which is different from the traditional way of pulse-SAR signal processing. This distinction makes the passive jamming method variational, and some new passive jamming methods should be studied.

In this paper, the model of rotary target's echo signal for FMCW SAR is established. The jamming characteristics of rotary target for FMCW SAR imaging is analyzed first, and then the parameter setting of rotary corner reflectors is discussed in detail. In this way, a passive suppressing jamming method for FMCW SAR adopting rotary corner reflectors is proposed. Finally, the simulation results verified the effectiveness of the proposed method.

## 2. JAMMING SIGNAL MODEL

The geometry model of FMCW SAR is illustrated in Fig. 1, where the carrier aircraft moves along the $x$ axis direction with speed $v$ and flight height $h$. Suppose that there is a rotary target point $P$ in the azimuth center, with rotary radius $r$, rotary frequency $f_P$ (angular frequency $\omega_P = 2\pi f_P$), initial phase $\theta_0$ and distance $R_0$ from the rotation center to radar platform.

The long duration of pulse makes the conventional "stop and go" approximation fail for FMCW SAR signal processing, and the change of range caused by the continuous movement of platform should be considered. Therefore, the instantaneous slant distance between rotary point $P$ and carrier aircraft can be represented as

$$R(t) \approx R_0 + r\cos\left(\omega_P t + \theta_0\right) + \frac{\left(vt - r\sin\left(\omega_P t + \theta_0\right)\right)^2}{2R_0} \tag{1}$$

Among them, $t = t_k + t_m$ represents the total time, and $t_k$, $t_m$ represent fast time and slow time, respectively. Further expand Eq. (1) as

$$R(t) \approx R\left(t_m\right) - \omega_P r\sin\left(\omega_v t_m + \theta_0\right) t_k + \frac{v^2 t_m}{R_0} t_k \tag{2}$$

where

$$R\left(t_m\right) \approx R_0 + r\cos\left(\omega_P t_m + \theta_0\right) + \frac{\left(vt_m - r\sin\left(\omega_P t_m + \theta_0\right)\right)^2}{2R_0} \tag{3}$$

In Eq. (2), the second term is the change of range in pulse duration caused by the rotary point, and the third term is the Doppler shift caused by continuous movement of aircraft. In the subsequent

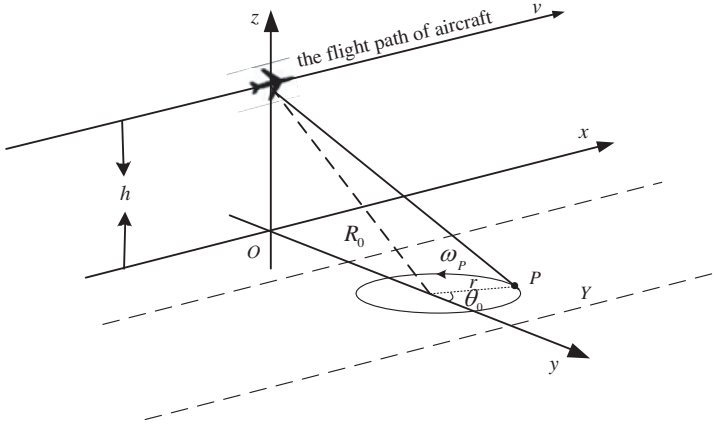


**Figure 1.** The geometry model of FMCW SAR.

processing, the Doppler shift can be compensated by constructing compensation function in azimuth Doppler domain.

After the "dechirp" processing of echo signals, the difference-frequency signal can be expressed by

$$s(t_k, t_m) = \sigma_P \exp\left(-j\left(\frac{4\pi\mu}{c}\left(t_k - \frac{2R_{ref}}{c}\right)R_\Delta(t) + \frac{4\pi}{\lambda}R_\Delta(t)\right)\right)\exp\left(j\frac{4\pi\mu}{c^2}R_\Delta^2(t)\right) \tag{4}$$

where $\sigma_P$ is the scattering coefficient of rotary point $P$, $c$ the speed of light, $\lambda$ the wavelength and $R_\Delta(t) = R(t) - R_{ref}$ ($R_{ref}$ the reference distance). The last term of Eq. (4) is residual video phase (RVP), whose compensation can be achieved in azimuth Doppler domain [8]. In this paper, the effect of RVP is ignored in the subsequent analysis. Combined with Eq. (2), we can get

$$\begin{aligned} s(t_k, t_m) \;=\; & \sigma_P \exp\left(-j\left(\frac{4\pi\mu}{c}R_\Delta\left(t_m\right)t_k - \frac{4\pi}{\lambda}\omega_P r\sin\left(\omega_v t_m + \theta_0\right)t_k\right)\right) \\ & \cdot\exp\left(-j\frac{4\pi}{\lambda}R_\Delta\left(t_m\right)\right)\exp\left(-j\frac{4\pi v^2 t_m}{\lambda R_0}t_k\right) \end{aligned} \tag{5}$$

where the first term is range imaging factor; the second term is azimuth imaging factor; the third term is the Doppler shift caused by continuous movement of carrier aircraft, a coupling term of fast time and slow time. The compensation of Doppler shift should be completed in azimuth Doppler domain. Conduct Fourier transform in terms of $t_m$ to Eq. (5) and construct Doppler shift compensation function as

$$H_D\left(t_k, f_a\right) = \exp\left(-j2\pi f_a t_k\right) \tag{6}$$

where $f_a$ represents azimuth Doppler frequency. After the Doppler shift compensation, taking the inverse Fourier transform in terms of $f_a$, it can be obtained that

$$s(t_k, t_m) = \sigma_P \exp\left(-j\left(\frac{4\pi\mu}{c}R_\Delta\left(t_m\right)t_k - \frac{4\pi}{\lambda}\omega_P r\sin\left(\omega_v t_m + \theta_0\right)t_k\right)\right)\cdot\exp\left(-j\frac{4\pi}{\lambda}R_\Delta\left(t_m\right)\right) \tag{7}$$

## 3. JAMMING CHARACTERISTICS ANALYSIS AND PARAMETER DESIGN

In this paper, take the Range-Doppler (R-D) algorithm as an example, the jamming characteristics of rotary target for FMCW SAR is analyzed. Conduct distance compression processing first, that is to conduct Fourier transform in terms of fast time to Eq. (7) and get

$$S\left(f_r, t_m\right) = \sigma_P \mathrm{sinc}\left(T_P\left(f_r + \psi\left(t_m\right)\right)\right)\exp\left(-j\frac{4\pi R\left(t_m\right)}{\lambda}\right) \tag{8}$$

$$\begin{aligned} \psi\left(t_m\right) \;=\; & \frac{2\mu}{c}R_\Delta\left(t_m\right) - \frac{2}{\lambda}\omega_P r\sin\left(\omega_v t_m + \theta_0\right) \\ =\; & \frac{2\mu}{c}\left(R_0 - R_{ref} + r\cos\left(\omega_P t_m + \theta_0\right) - \frac{\omega_P r f_c}{\mu}\sin\left(\omega_v t_m + \theta_0\right)\right) \\ =\; & \frac{2\mu}{c}\left(R_0 - R_{ref} + A\cos\left(\omega_P t_m + \varphi\right)\right) \end{aligned} \tag{9}$$

where $A = \sqrt{r^2 + a^2}$, $a = \omega_P r f_c/\mu$, $\varphi = \arctan\left(a/r\right) + \theta_0$ and $f_c$ is the carrier frequency. When $A > \rho_r$, the rotary point appears in the form of sine (cosine) term in range-slow time spectrogram, and the range shift $A$ (also called equivalent rotary radius) is related to not only the actual rotary radius but also parameters such as rotary frequency and carrier frequency. In order to achieve passive suppressing jamming, the parameters of corner reflectors are usually set to make the equivalent rotary radius cover a certain extent of range and form jamming stripes. Fig. 2 illustrates the relation curve between rotary frequency and equivalent rotary radius, where the carrier frequency of FMCW SAR is 35 GHz, the bandwidth 300 MHz, the pulse repetition time 1 ms and the corresponding pulse repetition frequency (PRF) 1000 Hz. It can be seen that with the increase of rotary frequency, the equivalent rotary radius increases accordingly.

For static point target, after range compression the echo signal is shown as a line in range-slow time spectrogram. After range migration correction, the line can be corrected into a single range cell.

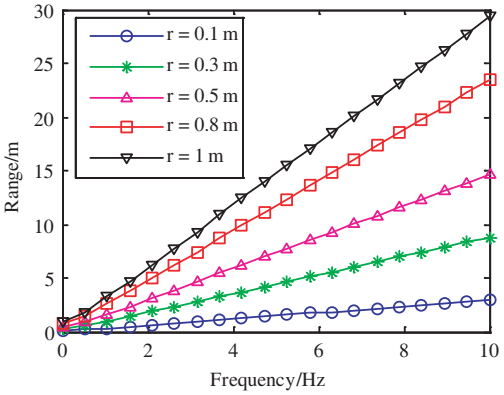


**Figure 2.** The relation curve between rotary frequency and equivalent rotary radius.

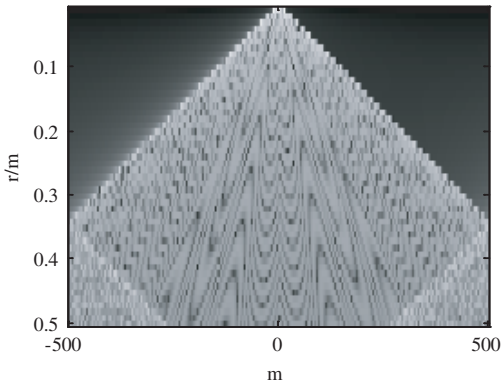


**Figure 3.** The Amplitude of $J_m(B)$.

After azimuth compression, the two-dimensional imaging result of the point can be obtained. However, due to the effect of rotation, there is sinusoidal phase modulation in the echo signal. After azimuth compression, the echo signal can be expressed by

$$S\left(f_r, t_m\right) = \sigma_P \text{sinc}\left(T_P\left(f_r + \psi\left(t_m\right)\right)\right) \sum_{m=-\infty}^{\infty} J_m\left(B\right) \text{sinc}\left(t_m + \frac{m f_P}{k_a}\right) \tag{10}$$

where $k_a = -2v^2/\lambda R_0$ is the azimuth Doppler Chirp rate, $B = 4\pi r/\lambda$, and $J_m\left(B\right)$ is Bessel function of the first kind [12], whose expression is

$$J_m\left(B\right) = \frac{1}{2\pi} \int_{-\pi}^{\pi} \exp\left(-B\cos\left(x + \theta_0\right)\right) e^{jmx} dx \tag{11}$$

According to Eq. (10), after azimuth compression the echo signal of rotary point target is the superposition of a series of narrow pulse signals. The interval between adjacent narrow pulses is

$$\Delta t = \frac{f_P}{k_a} \tag{12}$$

The value domain of the number of narrow pulses, $m$, is determined by Bessel function $J_m(B)$. Conduct variable substitution $x = -2\pi x'$ on Eq. (11), we can get

$$\begin{aligned} J_m\left(B\right) &= \frac{1}{2\pi} \int_{-\pi}^{\pi} \exp\left(-B\cos\left(-2\pi x' + \theta_0\right)\right) e^{-j2\pi m x'} d\left(-2\pi x'\right) \\ &= -\int_{-\pi}^{\pi} \exp\left(-B\cos\left(-2\pi x' + \theta_0\right)\right) e^{-j2\pi m x'} dx' \end{aligned} \tag{13}$$

To avoid confusing, Eq. (13) is still written as

$$J_m\left(B\right) = -\int_{-\pi}^{\pi} \exp\left(-B\cos\left(-2\pi x + \theta_0\right)\right) e^{-j2\pi m x} dx \tag{14}$$

According to Eq. (14), $J_m(B)$ is actually Fourier transform of a sinusoidal frequency modulation signal, whose bandwidth is the value domain of $m$, that is

$$m \in (-B, B) \tag{15}$$

With radar parameters fixed, the number of narrow pulses is determined by the rotary radius. Fig. 3 provides diagram of the amplitude of $J_m(B)$ with different $m$ and rotary radius $r$. It can be seen that with the increase of rotary radius, the number of narrow pulses increases accordingly. When rotary radius is more than 0.34 m, the bandwidth of $J_m(B)$ exceeds 500 Hz, i.e., $PRF/2$. Now the number of narrow pulses will no longer increase according to Nyquist sampling law.

According to the above analysis of rotary target's jamming characteristics for FMCW SAR, rotary corner reflectors can be used to implement passive suppressing jamming through generating two-dimensional jamming strips in range and azimuth. The jamming in azimuth is mainly achieved by narrow pulses formed after the azimuth compression of rotary corner reflector echo signal, where the interval of narrow pulses determines the jamming performance. In order to ensure that narrow pulses can cover the entire azimuth, i.e., $\Delta x < \rho_a$, where $\rho_a$ is the azimuth resolution, the rotary frequency of corner reflector should satisfy

$$\frac{f_P}{k_a PRI} \leq \frac{1}{k_a T_s PRI}, \quad \text{i.e.,} \quad f_P \leq \frac{1}{T_s} \tag{16}$$

The range of azimuth jamming is determined by the interval and number of narrow pulses. According to the interval of narrow pulse, the number of narrow pulses needed to form $L_a$ range of jamming in azimuth is

$$k_m \geq \frac{L_a}{\Delta x} = \frac{L_a f_P T_s}{\rho_a} \tag{17}$$

where $T_s$ is synthetic aperture time. Since the number of narrow pulses satisfies

$$k_m = \text{floor}\{2B\} = \text{floor}\{8\pi r/\lambda\} \tag{18}$$

where floor$\{\cdot\}$ means to round down. Then the rotary radius can be determined by

$$r \geq \frac{k_m \lambda_m}{8\pi} \tag{19}$$

With rotary frequency and rotary radius fixed, the equivalent rotary radius can be written by $A = \sqrt{r^2 + a^2}$. With range jamming extent $L_r$, the number of rotary corner reflectors $k_n$ should satisfy

$$k_n \geq \frac{L_r}{2A} \tag{20}$$

## 4. SIMULATION AND ANALYSIS

Suppose that the carrier frequency of FMCW SAR is 35 GHz, the bandwidth 300 MHz, the pulse duration 1 ms and the sampling frequency 1.25 MHz. FMCW SAR is working in side-looking mode. The speed of aircraft is 200 m/s, the distance from the center of target area to aircraft 5 km, the synthetic aperture time 0.21 s, and range and azimuth resolution are both 0.5 m.

### 4.1. Analysis of Jamming Characteristics

The jamming characteristics of rotary target are simulated and analyzed first, where the parameter settings of rotary point are shown in Table 1.

**Table 1.** Parameter settings of rotary corner reflectors.

| Corner reflector index | | 1 | 2 | 3 | 4 | 5 |
|---|---|---|---|---|---|---|
| Parameter setting 1 | $r$ (m) | 0.01 | 0.02 | 0.03 | 0.04 | 0.05 |
| | $f_P$ (Hz) | 5 | 5 | 5 | 5 | 5 |
| | location (km) | (0, 4.9) | (0, 4.95) | (0, 5) | (0, 5.05) | (0, 5.1) |
| Parameter setting 2 | $r$ (m) | 0.2 | 0.2 | 0.2 | 0.2 | 0.2 |
| | $f_P$ (Hz) | 1 | 2 | 5 | 20 | 40 |
| | location (km) | (0, 4.9) | (0, 4.95) | (0, 5) | (0, 5.05) | (0, 5.1) |

Figure 4 illustrates the FMCW SAR imaging results of rotary target adopting R-D algorithm with different parameter settings. With parameter setting 1, the equivalent rotary radiuses of 5 rotary corner reflectors are 0.038 m, 0.076 m, 0.114 m, 0.152 m and 0.190 m, respectively, all of which are smaller

than range resolution, thus forming line along with the azimuth direction in the imaging results. The rotary frequencies of 5 corner reflectors are the same, which brings the same narrow pulse interval in imaging results. Meanwhile, with the increase of rotary radius, the number of narrow pulses increase accordingly, which means more jamming strips in imaging. Under the condition of parameter setting 2, with different rotary frequencies and the same rotary radius of corner reflectors, the equivalent rotary radiuses are different, which are 0.25 m, 0.35 m, 0.76 m, 2.94 m and 5.87 m, respectively. Number 1, 2 corner reflectors' equivalent rotary radiuses are still smaller than range resolution; therefore, their imaging results are represented as lines along the azimuth direction, while those of numbers 3–5 are larger than range resolution, which brings strips along the azimuth direction in imaging.

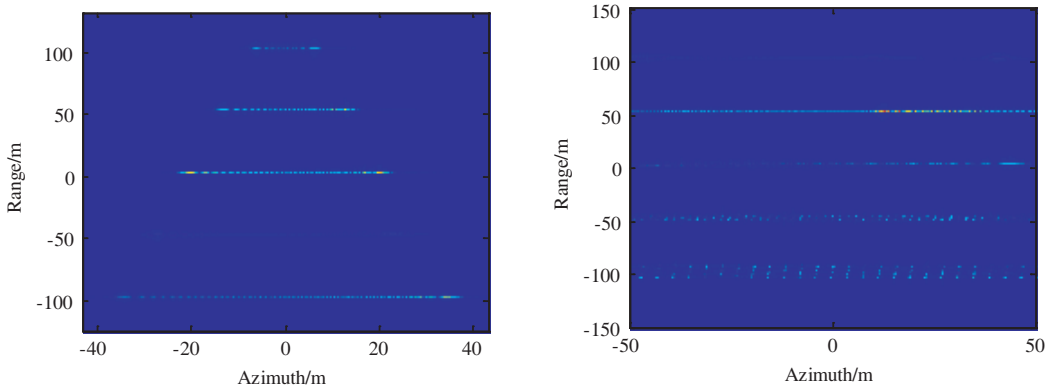


**Figure 4.** Analysis of jamming characteristics. (a) Parameter setting 1. (b) Parameter setting 2.

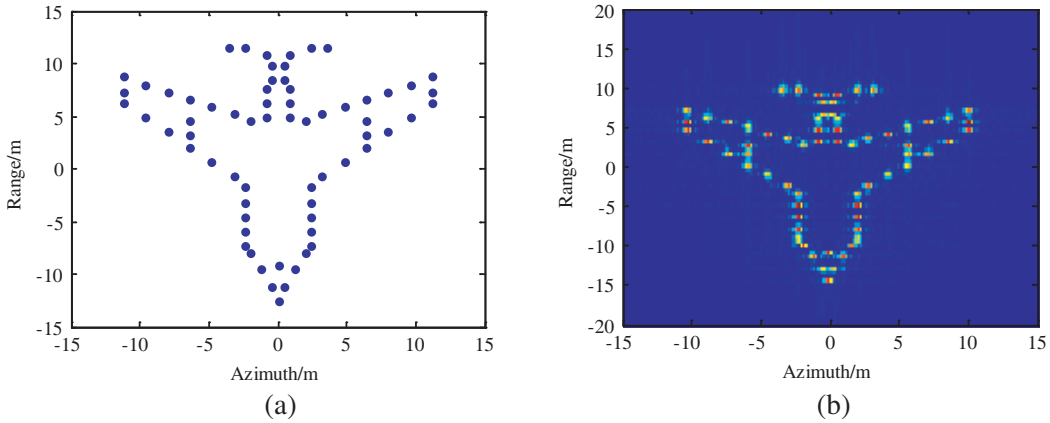


**Figure 5.** The model of the screened target. (a) Airplane model of 66 scatterers. (b) Two-dimensional imaging results.

### 4.2. Analysis of Jamming Performance

Take airplane model of 66 scatterers as the model of screened target, as shown in Fig. 5(a), and whose two-dimensional imaging result without jamming is shown in Fig. 5(b).

According to theoretical analysis result and the size of screened target, different parameter settings can be adopted to ensure effective screening. The parameter setting of rotary corner reflectors is shown in Table 2. The scattering coefficient of corner reflectors is 30 times that of target point. Fig. 6 provides imaging results of FMCW SAR with passive suppressing jamming implemented under conditions of different rotary corner reflector parameter settings.

**Table 2.** Parameter settings of rotary corner reflectors.

| Corner reflectors | Parameter setting 1 | Parameter setting 2 | Parameter setting 3 | Parameter setting 4 |
|---|---|---|---|---|
| $r$ (m) | 1.62 | 1 | 1.05 | 1.35 |
| $f_P$ (Hz) | 10 | 8 | 5 | 2 |
| number of reflectors | 1 | 2 | 3 | 5 |

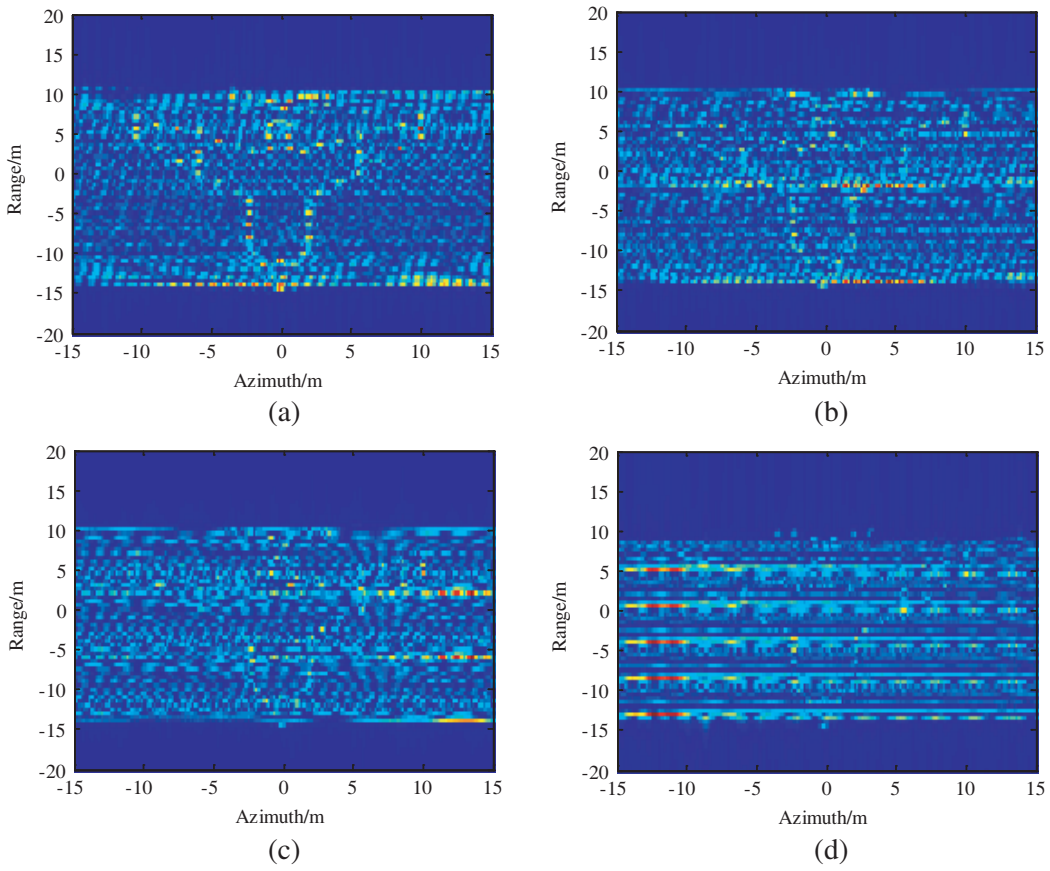


**Figure 6.** Imaging results with jamming implemented. (a) Parameter setting 1. (b) Parameter setting 2. (c) Parameter setting 3. (d) Parameter setting 4.

The parameter settings can all basically make range jamming strips cover the entire screened target. With the rotary frequency decreasing, the interval of narrow pulses formed in azimuth decreases accordingly, thus creating better azimuth jamming performance. With parameter setting 4, the screened airplane is totally submerged in the noise of corner reflector echo signal. The signal-to jamming (SJR) ratio are $-11.22$ dB, $-14.23$ dB, $-15.99$ dB and $-18.19$ dB, respectively.

In practicable applications, appropriate parameter settings of corner reflectors can be adopted according to the specific condition of screened target to better the performance of passive suppressing jamming for FMCW SAR.

## 5. CONCLUSION

Due to the FMCW SAR's own superiority, it will definitely catch more and more attention, and the jamming to FMCW SAR will increasingly become a hotspot in research of jamming technology. In this paper, the jamming characteristics of rotary target for FMCW SAR is analyzed, and a passive suppressive jamming method for FMCW SAR based on micro motion modulation is proposed. This method makes use of the rotary corner reflectors to form jamming strips in range and azimuth, thus realizing effective protection of the screened targets. The simulations validate the theoretical derivation and the effectiveness of the proposed passive supressing jamming method.

## ACKNOWLEDGMENT

This work was supported in part by the National Natural Science Foundation of China under Grant 61471386 and the Coordinator innovative engineering project of Shaanxi province under Grant 2015KTTSGY04-06.

## REFERENCES

1. Meta, A. and P. Hoogeboom, "Development of signal processing algorithms for high resolution airborne millimeter wave FMCW SAR," *Proc. IEEE Int. Radar Conf.'05*, 326–331, Arlington, U.S.A, 2005.
2. Meta, A., P. Hoogeboom, and L. P. Ligthart, "Signal processing for FMCW SAR," *IEEE Transactions on Geoscience and Remote Sensing*, Vol. 45, No. 11, 3519–3532, 2007.
3. Wang, R., Y. Luo, Y. Deng, et al., "Motion compensation for high-resolution automobile FMCW SAR," *IEEE Geoscience and Remote Sensing Letters*, Vol. 10, No. 5, 1157–1161, 2013.
4. Liu, Y., Y. Deng, R. Wang, et al., "Efficient and precise frequency-modulated continuous wave synthetic aperture radar raw signal simulation approach for extended scenes," *IET Radar Sonar and Navigation*, Vol. 6, No. 9, 858–866, 2012.
5. Adve, R., "Bistatic FMCW SAR signal model and imaging approach," *IEEE Transactions on Aerospace and Electronics*, Vol. 49, No. 3, 2017–2028, 2013.
6. Edrich, M., "Design overview and flight test results of the miniaturized SAR sensor MISAR," *Proc. EuRAD'04*, 205–208, Amsterdam, The Netherlands, 2004.
7. Duersch, M. I., "BYU. Micro-SAR: A very small low-power LFM-CW synthetic aperture radar," Brigham Young University, 2004.
8. Wang, R., O. Loffeld, H. Nies, et al., "Focus FMCW sar data using the wavenumber domain algorithm," *IEEE Transactions on Geoscience and Remote Sensing*, Vol. 48, No. 4, 2109–2118, 2010.
9. Sun, G.-C., X.-R. Bai, F. Zhou, et al., "A new passive barrage jamming method for SAR," *Journal of Electronics & Information Technology*, Vol. 31, No. 3, 610–613, 2009 (in Chinese).
10. Wu, X.-F., D.-H. Dai, X.-S. Wang, et al., "A novel method of active jamming for SAR based on micro motion modulation," *Acta Electronica Sinica*, Vol. 38, No. 4, 954-958, 2010 (in Chinese).
11. Wu, X.-F., Y. Liu, X.-S. Wang, et al., "Analysis of SAR imaging characteristics of targets with rotational micro-motion," *Journal of Astronautics*, Vol. 31, No. 4, 1181–1189, 2010 (in Chinese).
12. Rigling, B. D., "Image-quality focusing of rotary SAR targets," *IEEE Geosci. Remote Sens. Lett.*, Vol. 5, No. 4, 750–754, Oct. 2008.